

Thermo- and Acid-Responsive Photochromic Spiroanthoxazine-Containing Organogelators

Yongguang Li,^[a] Keith Man-Chung Wong,^[b] Anthony Yiu-Yan Tam,^[b] Lixin Wu,^[a] and Vivian Wing-Wah Yam^{*[a, b]}

Abstract: A series of photochromic spiroanthoxazine derivatives has been designed, synthesized, and characterized by using ¹H NMR spectroscopy, FAB mass spectrometry, and elemental analysis. Their photophysical and photochromic behavior have been investigated. Two of the compounds (G¹²-en-SA-SO and G¹⁶-en-SA-SO) have been shown to be capable of forming stable thermoreversible organogels in organic solvents, tested by the “stable-to-inversion of a test tube” method. Addition

of *p*-toluenesulfonic acid was found to induce the formation of stable organogels at concentrations below that of the critical gelation concentration (c.g.c.), with a concomitant change in color from colorless to purple. Transmission electron microscopy and scanning elec-

tron microscopy of the xerogels showed typical fibrous structures in the micrometer scale. The activation parameters for the bleaching reaction of G⁸-en-SA-SO in the solution state and G¹⁶-en-SA-SO in the gel state have been determined in ethanol through kinetic studies at various temperatures. The results showed that the rate of the bleaching reaction in the gel state was much slower than that in the solution state.

Keywords: acidichromism • organogels • photochromism • spiroanthoxazine • supramolecular chemistry

Introduction

During the past few decades, there has been an increasing interest in the study of functional and stimuli-responsive organogels, as a result of their unique features and the increasing potential of the applications of soft matters as smart materials.^[1–3] Organogels consist of three-dimensional networks that are formed by self-assembly through noncovalent interactions, such as hydrogen bonding, hydrophobic–hydrophobic interactions, π – π stacking, and metal–ligand coordination. In the process of organogelation, the gelator molecules self-assemble through noncovalent interactions to form fibrous architectures on the nanometer scale, which, in turn, builds up a micrometer-scale entangled three-dimensional

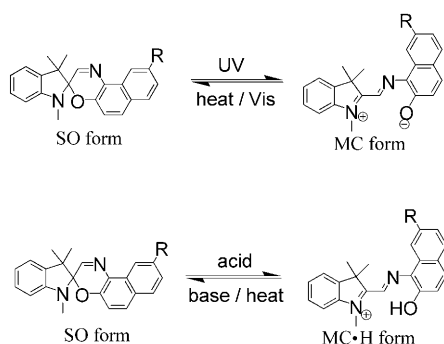
network entrapping/immobilizing organic solvent molecules, preventing the organic solvent molecules from flowing.

Smart gels, which show reversible changes in morphology or physical properties in response to various external stimuli, such as temperature, light, and pH, have previously been reported.^[4–11] Early examples include the pioneering works of Weiss in anthracene- and anthraquinone-based gelators.^[1a–c, f] Molecules exhibiting photochromic behavior have also been employed in the design of functional organogelators, including those of azobenzenes,^[2a, 5] diarylethenes,^[6, 7] spiropyran,^[8] and *2H*-chromenes.^[9] Apart from photochromic properties, organogelators based on *2H*-chromenes have also been shown to display acidichromic behavior.^[9a] Other acidichromic organogels have also been reported.^[10, 11]

Spirooxazines belong to another interesting class of materials that is known to show photochromic and acidichromic properties.^[12] Spirooxazines have also been shown to possess high fatigue resistance and excellent photo and pH stability.^[13] The photochromic behavior of spirooxazines, similar to spiropyran, has been attributed to the photochemical cleavage of the spiro carbon–oxygen bond that led to the planarization of the two originally orthogonal heterocycles, giving rise to an increase in the extent of π conjugation in the merocyanine (MC) structure, that is, the open form of the spirooxazine (Scheme 1). In addition, the spiro carbon–oxygen

[a] Y. Li, Prof. Dr. L. Wu, Prof. Dr. V. W.-W. Yam
State Key Laboratory of Supramolecular Structure and Materials
and College of Chemistry
Jilin University, Changchun 130012 (P.R. China)

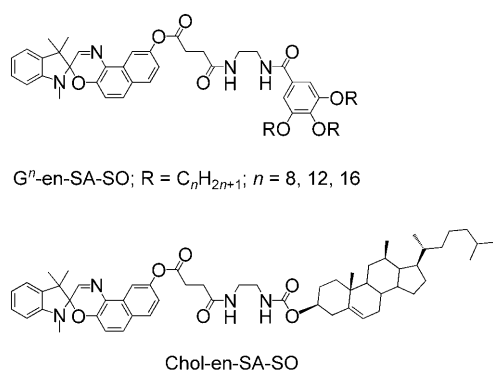
[b] Dr. K. M.-C. Wong, Dr. A. Y.-Y. Tam, Prof. Dr. V. W.-W. Yam
Institute of Molecular Functional Materials
and Department of Chemistry
The University of Hong Kong, Pokfulam Road (Hong Kong)
E-mail: wwyam@hku.hk



Scheme 1. Photo-induced (top) and proton-induced (bottom) ring-opening reactions of spironaphthoxazine.

bond could also be cleaved by acid to form another type of open form (MC·H) (Scheme 1).

Despite numerous studies on organic spiropyran, spirooxazines, and their transition metal complex systems known in solutions,^[14–16] corresponding studies on their photochromic organogels, as well as those of their related chromene systems are rare.^[8,9a] Herein, we report the synthesis, photo-physical, and photochromic properties of a series of spironaphthoxazine derivatives (Scheme 2). G¹²-en-SA-SO and



Scheme 2. Structures of spironaphthoxazine-containing molecules.

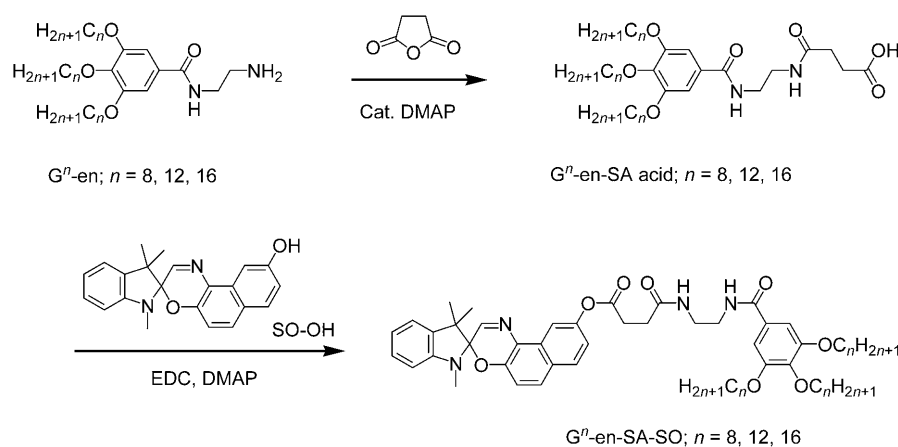
G¹⁶-en-SA-SO have been found to form stable thermotropic organogels in organic solvents at room temperature. Their gelation morphologies have been investigated by transmission electron microscopy (TEM) and scanning electron microscopy (SEM). Interestingly, while G¹²-en-SA-SO and G¹⁶-en-SA-SO could not form stable organogels in ethanol upon dilution to concentrations below that of their critical gelation concentration (c.g.c.), addition of *p*-toluenesulfonic acid could revive the

formation of stable organogels with the observation of a color change from colorless to purple.

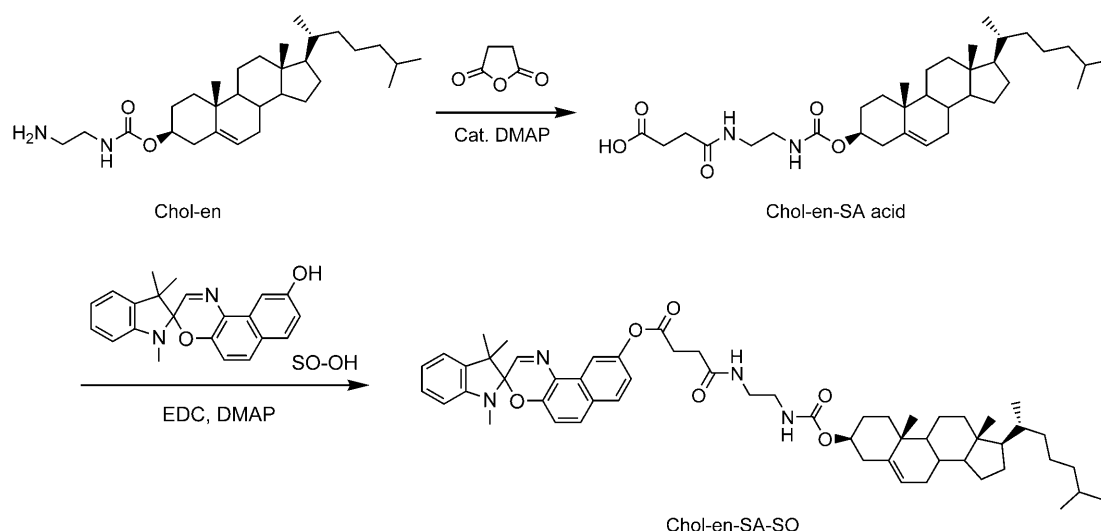
Results and Discussion

The synthetic routes for the preparation of the compounds, Gⁿ-en-SA-SO and Chol-en-SA-SO, are summarized in Schemes 3 and 4, respectively. Reactions of 1,3,3-trimethyl-9'-hydroxyspiroindolenine naphthoxazine (SO-OH) with *N*-[2-(3,4,5-trioctyloxybenzoylamino)ethyl]succinic acid (G⁸-en-SA acid), *N*-[2-(3,4,5-tridodecyloxybenzoylamino)ethyl]succinic acid (G¹²-en-SA acid), *N*-[2-(3,4,5-trihexadecyloxybenzoylamino)ethyl]succinic acid (G¹⁶-en-SA acid), or *N*-(2-cholesteryl aminoethyl)succinamic acid (Chol-en-SA acid) in the presence of 1-ethyl-3-(3-dimethylaminopropyl) carbodiimide hydrochloride (EDC) and 4-(dimethylamino)pyridine (DMAP) yielded the respective desired products in reasonably good yield. The Gⁿ-en-SA acids were prepared by several steps, involving the esterification of gallic acid with methanol, etherification with the corresponding alkyl bromides, ammonolysis of the obtained esters with ethylenediamine, followed by acylamidation with succinic anhydride. Chol-en-SA acid was prepared by reaction of cholesteryl chloroformate with ethylenediamine and then with succinic anhydride. All the intermediates were characterized by ¹H NMR spectroscopy. The final products were characterized by ¹H NMR spectroscopy, FAB mass spectrometry, and gave satisfactory elemental analysis.

The gelation properties of the compounds were tested in various organic solvents. It was found that Chol-en-SA-SO and G⁸-en-SA-SO could not form stable organogels in any organic solvents or mixed solvents. The probable reason for their lack of gelation properties may be attributed to the imbalance of the tendency of the gelator molecules to dissolve or to aggregate in organic solvents. On the contrary, both G¹²-en-SA-SO and G¹⁶-en-SA-SO have been found to show gelation properties in several organic solvents. The gelation properties are summarized in Table 1 and representative



Scheme 3. Synthetic routes for the preparation of Gⁿ-en-SA-SO.



Scheme 4. Synthetic routes for the preparation of Chol-en-SA-SO.

Table 1. Summary of gelation properties.

Organic solvent	G ¹² -en-SA-SO	G ¹⁶ -en-SA-SO
hexane	precipitate	gel ^[a] (1.0)
ethanol	gel ^[b] (15)	gel ^[a] (1.0)
acetone	gel ^[b] (15)	gel ^[a] (1.0)
DMF	sol	gel ^[a] (6.7)
DMSO	gel ^[a] (10)	gel ^[a] (2.1)

[a] The values in parentheses are the critical gelation concentrations in mg mL^{-1} at 20°C. [b] The values in parentheses are the critical gelation concentrations in mg mL^{-1} at 10°C.

photographs are shown in Figure 1a,b. The organogels in ethanol were found to turn blue in color upon UV irradiation. Upon exposure to visible light at room temperature, the color of the gels gradually returned back to colorless.

Interestingly, while G¹²-en-SA-SO ($1.1 \times 10^{-2} \text{ mol dm}^{-3}$) and G¹⁶-en-SA-SO ($6.9 \times 10^{-4} \text{ mol dm}^{-3}$) could not form stable organogels in ethanol solution upon dilution to concentrations below their respective c.g.c. ($1.3 \times 10^{-2} \text{ mol dm}^{-3}$ and $7.6 \times 10^{-4} \text{ mol dm}^{-3}$ respectively) (Figure 1c,d), addition of *p*-toluenesulfonic acid (2.8 mol L^{-1} , 1 μL and 0.35 mol L^{-1} , 1 μL) to the respective solutions led to the revival of stable organogel formation with the observation of a color change from colorless to purple. The re-formation of stable organogels required 1–2 h to complete at room temperature when the resultant solution was kept undisturbed. Acetic acid and hydrochloric acid could also induce the re-formation of the stable organogels in ethanol. The purple organogels could readily be destroyed by heating or upon the addition of an equimolar amount of triethylamine. Since UV irradiation could also induce similar ring-opening processes, an attempt to induce the re-formation of stable organogels by UV irradiation was made. Upon UV irradiation for 2 h at room temperature, the solution only showed a color change from colorless to blue and no stable organogel was formed during the UV irradiation. The lack

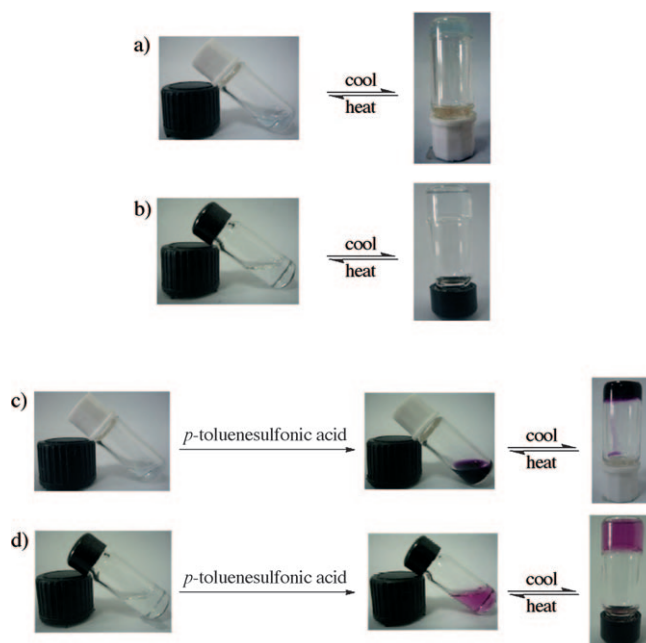


Figure 1. a) Photographs of ethanol sol (left) and gel (right) forms of G¹²-en-SA-SO ($1.3 \times 10^{-2} \text{ mol dm}^{-3}$). b) Photographs of ethanol sol (left) and gel (right) forms of G¹⁶-en-SA-SO ($9.1 \times 10^{-4} \text{ mol dm}^{-3}$). c) Photographs of ethanol sol form of G¹²-en-SA-SO ($1.1 \times 10^{-2} \text{ mol dm}^{-3}$) at concentrations below its c.g.c. (left) and the corresponding ethanol sol (middle) and gel (right) forms of G¹²-en-SA-SO ($1.1 \times 10^{-2} \text{ mol dm}^{-3}$) after the addition of equimolar amount of *p*-toluenesulfonic acid (2.8 mol L^{-1} , 1 μL). d) Photographs of ethanol sol form of G¹⁶-en-SA-SO ($6.9 \times 10^{-4} \text{ mol dm}^{-3}$) at concentrations below its c.g.c. (left) and the corresponding ethanol sol (middle) and gel (right) forms of G¹⁶-en-SA-SO ($6.9 \times 10^{-4} \text{ mol dm}^{-3}$) after the addition of equimolar amount of *p*-toluenesulfonic acid (0.35 mol L^{-1} , 1 μL).

of re-formation of stable organogels upon UV irradiation could probably be attributed to the very-fast rate of the thermal back reaction at room temperature that led to an

insufficient accumulation of the planar merocyanine (MC) form for the gelation process.

G^{12} -en-SA-SO and G^{16} -en-SA-SO were found to show different gelation abilities, attributed to the difference in length of the three alkoxy chains. G^{12} -en-SA-SO showed gelation properties in polar solvents, such as ethanol, acetone, and DMSO. The critical gelation temperature of G^{12} -en-SA-SO in ethanol and acetone was 10 °C, and the c.g.c. was $1.3 \times 10^{-2} \text{ mol dm}^{-3}$. It could form a gel in DMSO with a relatively lower c.g.c. ($8.7 \times 10^{-3} \text{ mol dm}^{-3}$) at 20 °C. However, it could only form a precipitate in nonpolar solvents such as hexane. In contrast, G^{16} -en-SA-SO could form organogels in both nonpolar solvents (e.g. hexane) and in polar solvents (e.g., ethanol, acetone) with a relatively lower c.g.c. ($7.6 \times 10^{-4} \text{ mol dm}^{-3}$) at 20 °C.

The morphology of the organogels was studied by TEM and SEM, and the images of their xerogels are shown in Figures 2 and 3. Both G^{12} -en-SA-SO and G^{16} -en-SA-SO showed fibrous structures upon self-assembly in the gel phase. The fibers undergo further cross-linking to form three-dimensional fibrous networks to entrap the solvent molecules.

The electronic absorption properties of G^8 -en-SA-SO in ethanol solution at 298 K were studied. The electronic absorption spectra showed a very intense absorption band at $\lambda = 280 \text{ nm}$, which was assigned to the $\pi \rightarrow \pi^*$ transitions of the indoline moiety. An additional absorption band was observed at $\lambda = 344 \text{ nm}$, which was assigned to the $\pi \rightarrow \pi^*$ transition of the naphthoxazine moiety. On prolonged excitation at $\lambda = 360 \text{ nm}$, the solution changed from colorless to blue. This was attributed to the photochromic reaction, in which the relatively weak spiro carbon–oxygen bond was photocleaved, resulting in the formation of the MC form (Scheme 1). The much lower energy absorption of MC at $\lambda = 600 \text{ nm}$ in the visible region was attributed mainly to the planarity of the two heterocyclic rings in the open form, resulting in an increase in the extent of π conjugation throughout the spiro-naphthoxazine moiety. However, these open forms were thermally unstable and would quickly undergo a bleaching reaction to the initial closed form.

As the organogel of G^{16} -en-SA-SO in ethanol exhibited a color change from colorless to blue upon UV irradiation, time-dependent electronic absorption changes of G^{16} -en-SA-SO

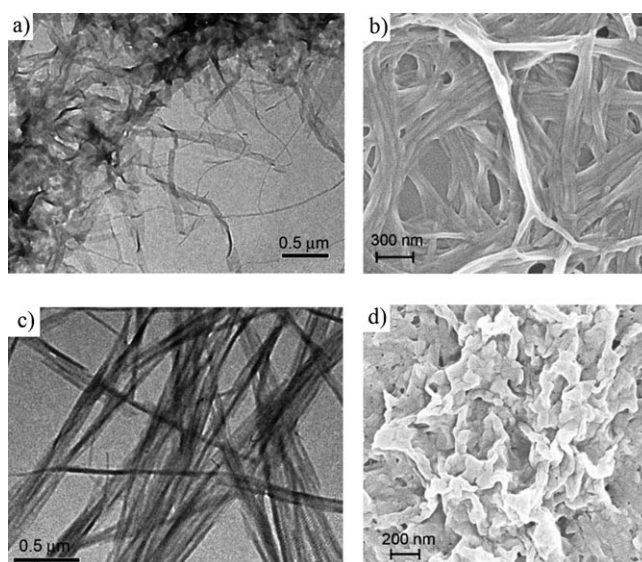


Figure 2. a) TEM and b) SEM images of the xerogels prepared from the ethanol gels of G^{16} -en-SA-SO. c) TEM and d) SEM images of the xerogels prepared from the hexane gels of G^{16} -en-SA-SO.

($9.1 \times 10^{-4} \text{ mol dm}^{-3}$) in ethanol gel with time intervals of 6 s at 10 °C in the dark after UV irradiation for 5 min were monitored. Upon UV irradiation at $\lambda = 360 \text{ nm}$, a new absorption band at $\lambda = 600 \text{ nm}$ appeared and reached its maximum rapidly, attributing to the formation of the photomero-

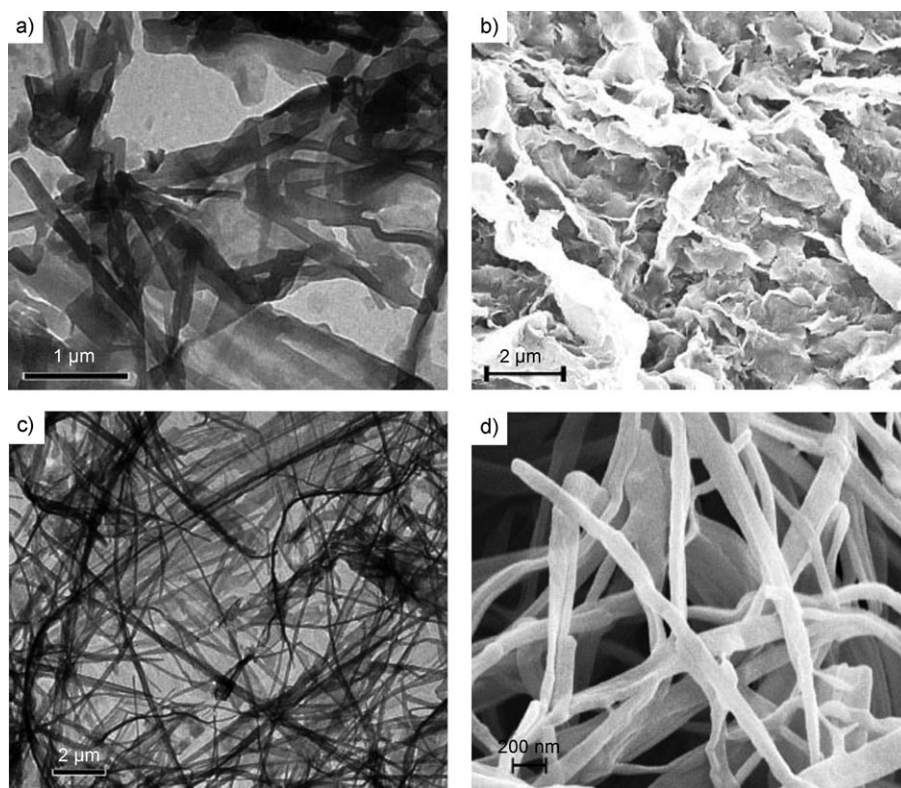


Figure 3. a) TEM and b) SEM images of the xerogels prepared from the DMSO gels of G^{16} -en-SA-SO. c) TEM and d) SEM images of the xerogels prepared from the DMSO gels of G^{12} -en-SA-SO.

cyanine form from the photochromic ring-opening reaction.^[14] After the irradiation, the gel was kept in the dark, and the new absorption band formed was found to drop rapidly with time and finally returned back to its original absorbance within 5 min as a result of the backward reaction of the photochromic reaction (Figure 4a).

The ethanol gel of G¹⁶-en-SA-SO could be readily destroyed upon dilution to concentrations below its c.g.c. ($7.6 \times 10^{-4} \text{ mol dm}^{-3}$). Interestingly, upon addition of an equimolar amount of *p*-toluenesulfonic acid ($6.9 \times 10^{-4} \text{ mol dm}^{-3}$, 3 μL) to an ethanol solution of G¹⁶-en-SA-SO ($6.9 \times 10^{-4} \text{ mol dm}^{-3}$), a stable organogel was found to form together with a drastic color change from colorless to purple. Time-dependent electronic absorption spectroscopy was used to trace this observation. Upon addition of *p*-toluenesulfonic acid, a new absorption band appeared at $\lambda = 550 \text{ nm}$ and reached its maximum within 2 h. The UV/Vis absorption spectral traces are shown in Figure 4b. The ability of

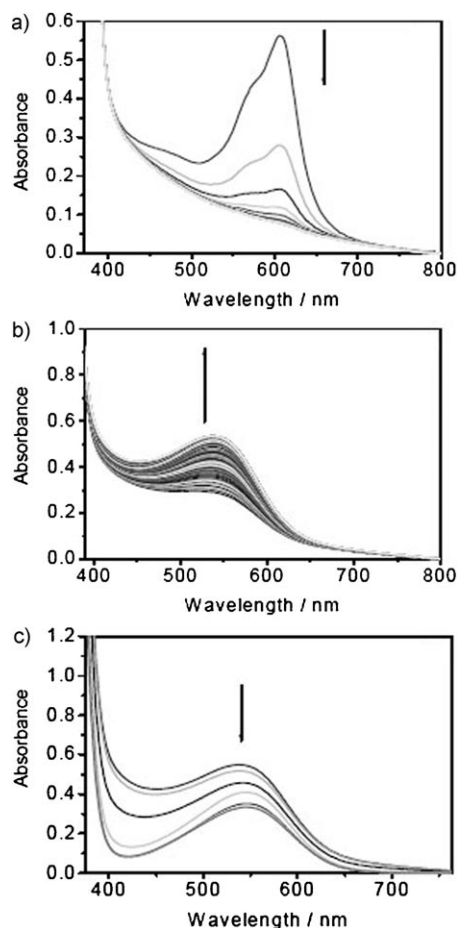


Figure 4. a) Time-dependent UV/Vis absorption spectral changes of G¹⁶-en-SA-SO ($9.1 \times 10^{-4} \text{ mol dm}^{-3}$) in ethanol with intervals of 6 s at 10°C in the dark after UV irradiation for 5 min. b) Time-dependent UV/Vis absorption spectral changes of G¹⁶-en-SA-SO ($6.9 \times 10^{-4} \text{ mol dm}^{-3}$) in ethanol with intervals of 6 s at 25°C upon the addition of equimolar amount of *p*-toluenesulfonic acid (0.69 mol dm^{-3} , 3 μL). c) Temperature-dependent UV/Vis spectral traces of G¹⁶-en-SA-SO ($6.9 \times 10^{-4} \text{ mol dm}^{-3}$) in ethanol from 25°C to 55°C with equimolar amount of *p*-toluenesulfonic acid added.

the organogel to re-form at concentrations below its c.g.c. in ethanol upon addition of *p*-toluenesulfonic acid has been ascribed to the lowering of the c.g.c. upon conversion of the nonplanar spiro structure (SO) into the planar protonated merocyanine (MC-H) form upon acid induced ring opening, which would increase the tendency for organogelation by means of the formation of π - π stacking interactions. The generation of the planar merocyanine form in the acid-induced organogel formation has been supported by the observation of an intense absorption band at $\lambda = 550 \text{ nm}$ in the UV/Vis study. The as-prepared purple gel was also subjected to a temperature-dependent UV/Vis absorption study. Upon increasing the temperature from 25 to 55°C, the $\lambda = 550 \text{ nm}$ absorption band decreased in intensity with a slight red shift in energy (Figure 4c), which indicates the thermal conversion of the protonated merocyanine (MC-H) form back to the spiro form.^[17] The higher energy of the absorption of the MC-H form at $\lambda = 550 \text{ nm}$ than that of the MC form at $\lambda = 600 \text{ nm}$ is consistent with the reduced extent of π conjugation of the ring opened merocyanine form upon protonation.

The kinetics for the bleaching reaction of the open form back to the closed form of G⁸-en-SA-SO (solution) and G¹⁶-en-SA-SO (gel) after excitation at $\lambda = 360 \text{ nm}$ in ethanol have been studied by using UV/Vis absorption spectroscopy at various temperatures. The thermal backward reaction resulted in the fading of the blue color and a decay of the low-energy absorption band (Figure 5). By monitoring the absorbance at $\lambda = 600 \text{ nm}$, the kinetics for the bleaching reactions were measured and the activation parameters were determined by using the Eyring and Arrhenius equations. The Eyring and Arrhenius plots are shown in Figure 6 and the activation parameters are summarized in Table 2. An activation energy (E_a) of $77.88 \text{ kJ mol}^{-1}$ was obtained for G¹⁶-en-SA-SO, which is higher than that of $62.47 \text{ kJ mol}^{-1}$ for G⁸-en-SA-SO, indicating that a higher activation energy is required for the ring-closing reaction of G¹⁶-en-SA-SO in the gel state than that of G⁸-en-SA-SO in the solution state.

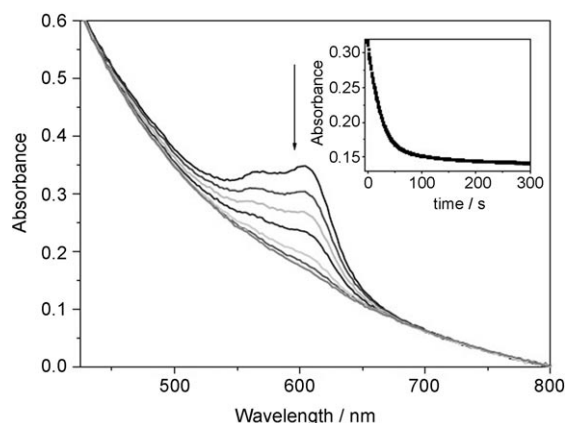


Figure 5. UV/Vis absorption spectral changes of G¹⁶-en-SA-SO ($9.1 \times 10^{-4} \text{ mol dm}^{-3}$, gel) in ethanol with intervals of 1 s at 20°C after excitation at $\lambda = 360 \text{ nm}$. The insert shows the absorption spectral trace at $\lambda = 600 \text{ nm}$ with time.

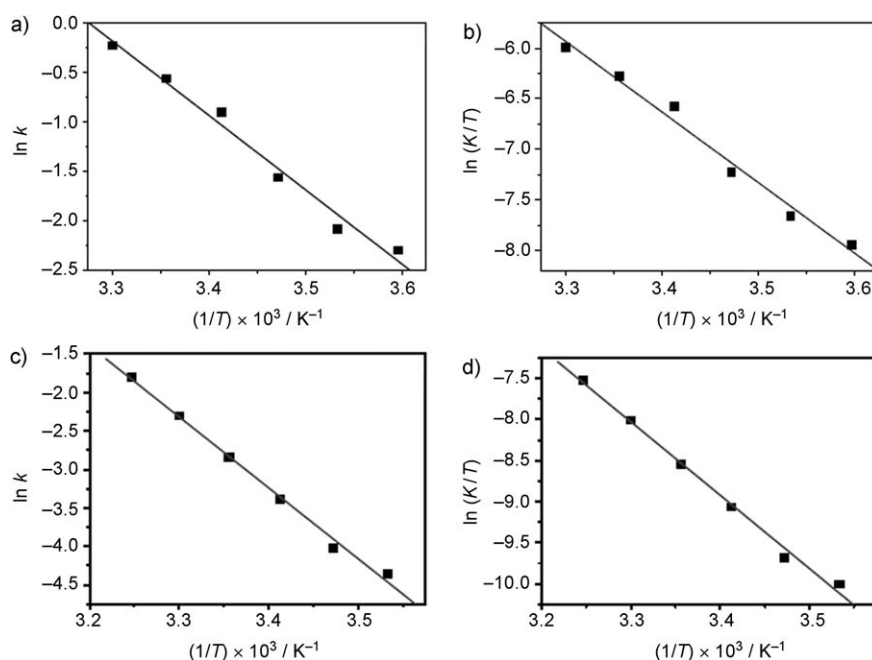


Figure 6. a) Arrhenius and b) Eyring plots for the thermal bleaching reaction of G^8 -en-SA-SO (sol) in ethanol. c) Arrhenius and d) Eyring plots for the thermal bleaching reaction of G^{16} -en-SA-SO (gel) in ethanol.

Table 2. Summary of the activation parameters for the bleaching reaction of the compounds in ethanol.

	G^8 -en-SA-SO ^[a]	G^{16} -en-SA-SO ^[b]
ΔH^\ddagger [kJ mol ⁻¹]	58.23	74.27
ΔS^\ddagger [J mol ⁻¹ K ⁻¹]	-54.66	-19.21
ΔG^\ddagger_{298K} [kJ mol ⁻¹]	74.52	79.99
E_a [kJ mol ⁻¹]	62.47	78.88
k [s ⁻¹]	283 K 298 K	0.133 0.058
		0.013 0.058

[a] Activation parameters were measured in the solution state. [b] Activation parameters were measured in the gel state.

The activation enthalpy (ΔH^\ddagger) of G^{16} -en-SA-SO (74.26 kJ mol⁻¹), which is larger than that of G^8 -en-SA-SO (58.23 kJ mol⁻¹), also suggested that the rate of bleaching reaction of G^{16} -en-SA-SO in the gel state is less favorable than that of G^8 -en-SA-SO in the solution state, consistent with the smaller bleaching rate constant for G^{16} -en-SA-SO than that of G^8 -en-SA-SO (Table 2). These results are also consistent with the observation that the ethanol solution of G^8 -en-SA-SO changed to colorless from blue immediately after switching off the UV light, whereas the ethanol gel of G^{16} -en-SA-SO turned to colorless gradually. As G^8 -en-SA-SO and G^{16} -en-SA-SO only differ in the chain length of the alkoxy chains, it is unlikely that such structural difference would lead to the large differences in the activation parameters. Thus the most probable reason for the large differences observed may be attributed to a difference in the viscosity of the medium. Given the rigidity of the medium in the gel state, it is not surprising that a larger activation energy would be required for the ring-closing reaction that involved

conformational structural change of the ethanol gel of G^{16} -en-SA-SO than the ethanol solution of G^8 -en-SA-SO.

Conclusion

In summary, a series of photochromic spironaphthoxazines of gallic acid and cholesterol derivatives has been synthesized and their photophysical and photochemical properties have been studied. G^{12} -en-SA-SO and G^{16} -en-SA-SO were shown to be capable of forming stable thermotropic organogels in organic solvents. A lowering of c.g.c. for organogel formation was observed upon addition of *p*-toluenesulfonic acid, concomitant with the growth of a low-energy colored band in the UV/Vis spectrum, owing to an acid-induced ring-opening process.

The activation parameters of the bleaching reaction of G^8 -en-SA-SO in the solution state and G^{16} -en-SA-SO in the gel state were determined in ethanol. The results showed that the rate of the bleaching reaction of the latter in the gel state is much slower than that of the former in the solution state, in line with the more restricted geometrical changes in the more viscous gel state.

Experimental Section

Materials and reagents: 2,7-Dihydronaphthalene and cholesteryl chloroformate were obtained from Aldrich Chemical Co. 1,3,3-Trimethyl-9'-hydroxy-spiroindolenaphthoxazine (SO-OH)^[18] and 3 β -cholesteryl-5-en-3-yl-*N*-(2-aminoethyl)carbamate (Chol-en)^[19] were prepared according to reported procedures. *N*-(2-Aminoethyl)-3,4,5-tris(octyloxy)benzamide (G^8 -en), *N*-(2-aminoethyl)-3,4,5-tris(dodecyloxy)benzamide (G^{12} -en), and *N*-(2-aminoethyl)-3,4,5-tris(hexadecyloxy)benzamide (G^{16} -en) were synthesized by modification of a reported procedure.^[20]

Synthesis

G^8 -en-SA acid: To a solution of succinic anhydride (85 mg, 0.85 mmol) and a catalytic amount of DMAP in $CHCl_3$ (50 mL) was added a solution of G^8 -en (470 mg, 0.85 mmol) in $CHCl_3$ (80 mL). The reaction mixture was heated to reflux for 2 h. The solvent was then removed under reduced pressure to afford the crude product, which was purified by column chromatography on silica gel using dichloromethane-acetone (2:1 v/v) in the presence of a few drops of HOAc to give the desired product. Yield: 446 mg, 81%. ¹H NMR (500 MHz, $CDCl_3$, 298 K, relative to TMS): δ = 0.89 (t, J = 6.7 Hz, 9H; -CH₃), 1.29–1.32 (m, 24H; -CH₂-), 1.44–1.50 (m, 6H; -CH₂-), 1.71–1.84 (m, 6H; -CH₂-), 2.49 (t, J = 6.2 Hz, 2H; -CH₂COO-), 2.66 (t, J = 6.2 Hz, 2H; -COCH₂-), 3.50–3.51 (m, 4H; -NCH₂CH₂N-), 3.98–4.03 (m, 6H; -OCH₂-), 6.75–6.77 (m, 1H; -NH-), 7.00 (s, 2H; -C₆H₂-), 7.06–7.07 ppm (m, 1H; -NH-).

G¹²-en-SA acid: The compound was synthesized by a procedure similar to that used for G⁸-en-SA acid, except that G¹²-en (609 mg, 0.85 mmol) was used instead of G⁸-en. The crude product was purified by column chromatography on silica gel using dichloromethane-acetone (4:1 v/v) in the presence of a few drops of HOAc to give the desired product. Yield: 597 mg, 86%. ¹H NMR (500 MHz, CDCl₃, 298 K, relative to TMS): δ = 0.88 (t, *J* = 6.8 Hz, 9H; -CH₃), 1.26–1.34 (m, 48H; -CH₂-), 1.44–1.50 (m, 6H; -CH₂-), 1.70–1.79 (m, 6H; -CH₂-), 2.47 (t, *J* = 6.3 Hz, 2H; -CH₂COO-), 2.66 (t, *J* = 6.3 Hz, 2H; -COCH₂-), 3.49–3.53 (m, 4H; -NCH₂CH₂N-), 3.98–4.00 (m, 6H; -OCH₂-), 6.81–6.85 (m, 1H; -NH-), 7.00 (s, 2H; -C₆H₂-), 7.19–7.21 ppm (m, 1H; -NH-).

G¹⁶-en-SA acid: The compound was synthesized by a procedure similar to that used for G⁸-en-SA acid, except that G¹⁶-en (751 mg, 0.85 mmol) was used instead of G⁸-en. The crude product was purified by column chromatography on silica gel using dichloromethane-hexane (2:1 v/v) in the presence of a few drops HOAc to give the desired product. Yield: 593 mg, 71%. ¹H NMR (500 MHz, CDCl₃, 298 K, relative to TMS): δ = 0.88 (t, *J* = 6.8 Hz, 9H; -CH₃), 1.26–1.30 (m, 72H; -CH₂-), 1.45–1.46 (m, 6H; -CH₂-), 1.72–1.81 (m, 6H; -CH₂-), 2.47 (t, *J* = 6.2 Hz, 2H; -CH₂COO-), 2.61 (t, *J* = 6.2 Hz, 2H; -COCH₂-), 3.49–3.52 (m, 4H; -NCH₂CH₂N-), 3.97–4.01 (m, 6H; -OCH₂-), 6.79–6.82 (m, 1H; -NH-), 7.00 (s, 2H; -C₆H₂-), 7.05–7.06 (m, 1H; -NH-).

G⁸-en-SA-SO: To a solution of G⁸-en-SA acid (325 mg, 0.5 mmol) and SO-OH (172 mg, 0.5 mmol) in dry dichloromethane (80 mL) was added a solution of EDC (192 mg, 1 mmol) and a catalytic amount of DMAP in dry dichloromethane (30 mL) under a nitrogen atmosphere and the reaction mixture was stirred at room temperature for overnight. The reaction mixture was washed with deionized water and the solvent was removed under reduced pressure. The crude product was purified by column chromatography on silica gel using dichloromethane-diethyl ether (3:1 v/v) to give the desired product. Yield: 280 mg, 59%. ¹H NMR (500 MHz, CDCl₃, 298 K, relative to TMS): δ = 0.88 (t, *J* = 6.8 Hz, 9H; -CH₃), 1.26–1.31 (m, 30H; -CH₂-), 1.39–1.48 (m, 6H; -CH₂-), 1.69–1.77 (m, 6H; -CH₂-), 2.64 (t, *J* = 6.7 Hz, 2H; -COCH₂-), 2.72 (s, 3H; -NCH₃), 2.99 (t, *J* = 6.7 Hz, 2H; -COCH₂-), 3.54–3.57 (m, 2H; -NCH₂-), 3.60–3.63 (m, 2H; -NCH₂-), 3.93–3.97 (m, 6H; -OCH₂-), 6.33 (t, *J* = 5.5 Hz, 1H; -NH-), 6.57 (d, *J* = 7.7 Hz, 1H; indolinic proton at 7-position), 6.90 (t, *J* = 7.7 Hz, 1H; indolinic proton at 5-position), 6.97 (d, *J* = 8.9 Hz, 1H; naphthoxazinic proton at 5'-position), 7.00 (s, 2H; -C₆H₂-), 7.06–7.12 (m, 3H; -NH-, indolinic proton at 4-position, naphthoxazinic proton at 8'-position), 7.22 (t, *J* = 7.7 Hz, 1H; indolinic proton at 6-position), 7.62 (d, *J* = 8.9 Hz, 1H; naphthoxazinic proton at 6'-position), 7.67 (s, 1H; naphthoxazinic proton at 2'-position), 7.70 (d, *J* = 8.9 Hz, 1H; naphthoxazinic proton at 7-position), 8.21 ppm (d, *J* = 2.1 Hz, 1H; naphthoxazinic proton at 10'-position); positive FAB-MS: *m/z*: 976 [M+H]⁺; elemental analysis (%) calcd for C₉₀H₉₆N₄O₈: C 72.64, H 8.48, N 5.75; found: C 72.52, H 8.67, N 5.48.

G¹²-en-SA-SO: The compound was synthesized by a procedure similar to that used for G⁸-en-SA-SO, except that G¹²-en-SA acid (166 mg, 0.2 mmol) was used instead of G⁸-en-SA acid. Yield: 81 mg, 35%. ¹H NMR (500 MHz, CDCl₃, 298 K, relative to TMS): δ = 0.88 (t, *J* = 7.0 Hz, 9H; -CH₃), 1.25–1.32 (m, 54H; -CH₂-), 1.40–1.46 (m, 6H; -CH₂-), 1.70–1.76 (m, 6H; -CH₂-), 2.64 (t, *J* = 6.6 Hz, 2H; -COCH₂-), 2.72 (s, 3H; -NCH₃), 2.99 (t, *J* = 6.6 Hz, 2H; -COCH₂-), 3.54–3.57 (m, 2H; -NCH₂-), 3.60–3.63 (m, 2H; -NCH₂-), 3.93–3.97 (m, 6H; -OCH₂-), 6.31 (t, *J* = 6.1 Hz, 1H; -NH-), 6.57 (d, *J* = 7.7 Hz, 1H; indolinic proton at 7-position), 6.90 (t, *J* = 7.7 Hz, 1H; indolinic proton at 5-position), 6.97 (d, *J* = 8.9 Hz, 1H; naphthoxazinic proton at 5'-position), 7.00 (s, 2H; -C₆H₂-), 7.06–7.10 (m, 3H; -NH-, indolinic proton at 4-position, naphthoxazinic proton at 8'-position), 7.21 (t, *J* = 7.7 Hz, 1H; indolinic proton at 6-position), 7.62 (d, *J* = 8.9 Hz, 1H; naphthoxazinic proton at 6'-position), 7.67 (s, 1H; naphthoxazinic proton at 2'-position), 7.70 (d, *J* = 8.9 Hz, 1H; naphthoxazinic proton at 7-position), 8.21 ppm (d, *J* = 2.4 Hz, 1H; naphthoxazinic proton at 10'-position); positive FAB-MS: *m/z*: 1143 [M+H]⁺; elemental analysis (%) calcd for C₇₁H₁₀₆N₄O₈: C 74.55, H 9.34, N 4.90; found: C 74.31, H 9.78, N 4.75.

G¹⁶-en-SA-SO: The compound was synthesized by a procedure similar to that used for G⁸-en-SA-SO, except that G¹⁶-en-SA acid (393 mg, 0.4 mmol) was used instead of G⁸-en-SA acid. Yield: 110 mg, 21%.

¹H NMR (500 MHz, CDCl₃, 298 K, relative to TMS): δ = 0.88 (t, *J* = 6.8 Hz, 9H; -CH₃), 1.25–1.34 (m, 78H; -CH₂-), 1.39–1.43 (m, 6H; -CH₂-), 1.69–1.77 (m, 6H; -CH₂-), 2.64 (t, *J* = 6.6 Hz, 2H; -COCH₂-), 2.72 (s, 3H; -NCH₃), 2.99 (t, *J* = 6.7 Hz, 2H; -COCH₂-), 3.56 (t, *J* = 5.0 Hz, 2H; -NCH₂-), 3.61 (t, *J* = 5.1 Hz, 2H; -NCH₂-), 3.93–3.96 (m, 6H; -OCH₂-), 6.31 (t, *J* = 5.2 Hz, 1H; -NH-), 6.57 (d, *J* = 7.7 Hz, 1H; indolinic proton at 7-position), 6.89 (t, *J* = 7.7 Hz, 1H; indolinic proton at 5-position), 6.97 (d, *J* = 8.9 Hz, 1H; naphthoxazinic proton at 5'-position), 7.00 (s, 2H; -C₆H₂-), 7.07–7.02 (m, 3H; -NH-, indolinic proton at 4-position, naphthoxazinic proton at 8'-position), 7.21 (t, *J* = 7.7 Hz, 1H; indolinic proton at 6-position), 7.62 (d, *J* = 8.9 Hz, 1H; naphthoxazinic proton at 6'-position), 7.67 (s, 1H; naphthoxazinic proton at 2'-position), 7.70 (d, *J* = 8.9 Hz, 1H; naphthoxazinic proton at 7-position), 8.21 ppm (d, *J* = 1.7 Hz, 1H; naphthoxazinic proton at 10'-position); positive FAB-MS: *m/z*: 1312 [M+H]⁺; elemental analysis (%) calcd for C₈₅H₁₃₀N₄O₈·2((C₂H₅)₂O): C 74.84, H 10.36, N 3.84; found: C 74.53, H 10.14, N 3.97.

Chol-en-SA acid: To a solution of succinic anhydride (258 mg, 2.8 mmol) and a catalytic amount of DMAP in CHCl₃ (50 mL) was added a solution of Chol-en (1.4 g, 2.8 mmol) in CHCl₃ (80 mL). The reaction mixture was heated to reflux for 2 h. The reaction mixture was then washed with 1 M HCl and deionized water and dried over anhydrous Na₂SO₄. Removal of the solvent under reduced pressure afforded the crude product. The crude product was dispersed in dichloromethane by sonication, and the product was filtered and washed with dichloromethane. Yield: 0.6 g, 38%. ¹H NMR (500 MHz, CDCl₃, 298 K, relative to TMS): δ = 0.68 (s, 3H; cholesteryl proton), 0.85–1.60 (m, 33H; cholesteryl proton), 1.79–2.02 (m, 5H; cholesteryl proton), 2.26–2.35 (m, 2H; cholesteryl proton), 2.54 (t, *J* = 6.4 Hz, 2H; -CH₂COO-), 2.70 (t, *J* = 6.4 Hz, 2H; -OCCH₂-), 3.33–3.40 (m, 4H; -NCH₂CH₂N-), 4.46–4.50 (m, 1H; -OCH-), 5.01 (m, 1H; -NH-), 5.38 (d, *J* = 5.1 Hz, 1H; -CH=C-), 6.66 ppm (m, 1H; -NH-).

Chol-en-SA-SO: To a solution of Chol-en-SA acid (286 mg, 0.5 mmol) and SO-OH (172 mg, 0.5 mmol) in dry dichloromethane was added a solution of EDC (190 mg, 1 mmol) and a catalytic amount of DMAP in dry dichloromethane under a nitrogen atmosphere, and the reaction mixture was stirred at room temperature for overnight. The reaction mixture was then washed with deionized water and the solvent was removed under reduced pressure. Purification by column chromatography on silica gel using dichloromethane-diethyl ether (1:3 v/v), followed by dichloromethane-acetone (4:1 v/v) gave the desired product. Further purification of the product was done by dispersing in MeCN by sonication, and the product was filtered and washed with MeCN. Yield: 230 mg, 51%. ¹H NMR (500 MHz, CDCl₃, 298 K, relative to TMS): δ = 0.66 (s, 3H; cholesteryl proton), 0.85–1.68 (m, 39H; cholesteryl proton and -(CH₂)₂), 1.76–2.00 (m, 5H; cholesteryl proton), 2.19–2.35 (m, 2H; cholesteryl proton), 2.62 (t, *J* = 6.8 Hz, 2H; -CH₂COO-), 2.75 (s, 3H; -NCH₃), 3.00 (t, *J* = 6.8 Hz, 2H; -CH₂COO-), 3.33–3.34 (m, 2, -NCH₂-), 3.41–3.43 (m, 2H; -NCH₂-), 4.44–4.49 (m, 1H; -OCH-), 5.08 (m, 1H; -NH-), 5.34 (d, *J* = 4.5 Hz, 1H; -CH=C-), 6.23 (m, 1H; -NH-), 6.57 (d, *J* = 7.7 Hz, 1H; indolinic proton at 7-position), 6.90 (t, *J* = 7.7 Hz, 1H; indolinic proton at 5-position), 6.98 (d, *J* = 8.9 Hz, 1H; naphthoxazinic proton at 5'-position), 7.08 (d, *J* = 7.7 Hz, 1H; indolinic proton at 4-position), 7.14 (d, *J* = 8.9 Hz, 1H; naphthoxazinic proton at 8'-position), 7.22 (t, *J* = 7.7 Hz, 1H; indolinic proton at 6-position), 7.64 (d, *J* = 8.9 Hz, 1H; naphthoxazinic proton at 6'-position), 7.71 (s, 1H; naphthoxazinic proton at 2'-position), 7.73 (d, *J* = 8.9 Hz, 1H; naphthoxazinic proton at 7-position), 8.22 ppm (d, *J* = 2.3 Hz, 1H; naphthoxazinic proton at 10'-position); positive FAB-MS: *m/z*: 900 [M+H]⁺; elemental analysis (%) calcd for C₅₆H₇₄N₄O₆·0.5((C₂H₅)₂O): C 74.39, H 8.51, N 5.99; found: C 74.13, H 8.89, N 6.04.

Physical measurements and instrumentation

NMR spectroscopy: ¹H NMR spectra were recorded by using a Bruker DRX 500 (500 MHz) spectrometer at 298 K. Chemical shifts (δ, ppm) were reported relative to tetramethylsilane (TMS). Positive ion FAB mass spectra were recorded by using a Finnigan MAT95 mass spectrometer. Elemental analyses of the compounds were performed by using a Flash EA 1112 elemental analyzer at the Changchun Institute of Applied Chemistry, Chinese Academy of Sciences.

Transmission electron microscopy and scanning electron microscopy: TEM experiments were performed by using a Philips Tecnai G2 20 S-

TWIN with an accelerating voltage of 200 kV. The TEM images were taken by using a Gatan MultiScan Model 794. SEM experiments were performed by using a Leo 1530 FEG operating at 4.0–6.0 kV. The TEM and SEM samples were prepared by dropping dilute gels onto a carbon-coated grid and a silicon wafer, respectively. Slow evaporation of solvents in air for 10 min led to xerogels. All the samples for SEM experiments were sputtered with gold thin film.

UV/Vis spectroscopy and photoirradiation: Time- and temperature-dependent electronic absorption spectra were obtained by using a Varian Cary 50 UV/vis spectrophotometer. The kinetics for the bleaching reaction were determined by measurement of the UV/Vis spectral changes at various temperatures with the use of a Hewlett–Packard 8452 A diode array spectrophotometer, with temperature controlled by a Lauda RM6 compact low-temperature thermostat. Photoirradiation was carried out by using a 300 W Xe (ozone-free) lamp (Oriol model 6258) and monochromatic light was obtained by passing the light through an Applied Photophysics F 3.4 monochromator. The thermal bleaching reaction of spironaphthoxazines is known to follow first-order kinetics at various temperatures. The first-order rate constants were obtained by taking the negative value of the slope of a linear least-squares fit of $\ln[(A - A_\infty)/(A_0 - A_\infty)]$ against time according to Equation (1):

$$\ln[(A - A_\infty)/(A_0 - A_\infty)] = -kt \quad (1)$$

in which A , A_0 , and A_∞ are the absorbance at the absorption wavelength maximum of the open form at times t , 0, and infinity, respectively, and k is the rate constant of the reaction. The kinetic parameters were obtained by a linear least-squares fit of $\ln(k/T)$ against $1/T$ according to the linear expression of the Eyring equation [Eq. (2)], $\ln k$ against $1/T$ according to the Arrhenius equation [Eq. (3)], and the changes in Gibbs free energy of activation (ΔG^\ddagger) at 298 K were determined according to Equation (4):

$$\ln(k/T) = -(\Delta H^\ddagger/R)(1/T) + \ln(k_B/h) + (\Delta S^\ddagger/R) \quad (2)$$

$$\ln(k) = -E_a/RT + \ln A \quad (3)$$

$$\Delta G^\ddagger = \Delta H^\ddagger - T\Delta S^\ddagger \quad (4)$$

in which ΔH^\ddagger and ΔS^\ddagger are the changes in enthalpy of activation and entropy of activation, respectively, E_a is the activation energy, T is the temperature, and k_B , R , h , and A are the Boltzmann's constant, the universal gas constant, the Planck constant, and the frequency factor, respectively.

Gelation test: The gelator and the solvent were placed in a screw-capped sample vial and the mixture was heated until the solid has dissolved. The sample vial was cooled, and was then left for 1 h at room temperature. The state of the materials was evaluated by the “stable-to-inversion of a test tube” method. Using G¹⁶-en-SA-SO as an example, 0.5 mg of the sample and 0.4 mL of ethanol were placed into the sample vial and the mixture was heated to 50 °C until all of the solid dissolved. The sample vial was cooled to 20 °C and was left for 1 h undisturbed. A stable thermoreversible organogel was formed, and the gelation was evaluated by the “stable-to-inversion of a test tube” method.

Acknowledgements

V.W.-W.Y. acknowledges support from The University of Hong Kong under the Distinguished Research Achievement Award Scheme. We also acknowledge support from Jilin University and the University of Hong Kong. This work has been supported by the Areas of Excellence Scheme, University Grants Committee (Hong Kong) (work at the Institute of Molecular Materials; grant no. AoE/P-03/08) and the Natural Science Foundation of China and the Research Grants Council of Hong Kong Joint Research Scheme (NSFC-RGC Project No. N_HKU 737/06). A.Y.-Y.T. acknowledges the receipt of a University Postdoctoral Fellowship from The University of Hong Kong.

- [1] a) Y. Lin, R. G. Weiss, *Macromolecules* **1987**, *20*, 414; b) I. Furmant, R. G. Weiss, *Langmuir* **1993**, *9*, 2084; c) R. Mukkamala, R. G. Weiss, *Langmuir* **1996**, *12*, 1474; d) P. Terech, R. G. Weiss, *Chem. Rev.* **1997**, *97*, 3133; e) D. J. Abdallah, R. G. Weiss, *Adv. Mater.* **2000**, *12*, 1237; f) L. Lu, T. M. Cocker, R. E. Bachman, R. G. Weiss, *Langmuir* **2000**, *16*, 20.
- [2] a) K. Murata, M. Aoki, T. Suzuki, T. Harada, H. Kawabata, T. Komri, F. Olrseto, K. Ueda, S. Shinkai, *J. Am. Chem. Soc.* **1994**, *116*, 6664; b) K. Sugiyasu, N. Fujita, S. Shinkai, *Angew. Chem.* **2004**, *116*, 1249; *Angew. Chem. Int. Ed.* **2004**, *43*, 1229; c) T. Kitahara, M. Shirakawa, S. Kawano, U. Beginn, N. Fujita, S. Shinkai, *J. Am. Chem. Soc.* **2005**, *127*, 14980; d) N. Fujita, Y. Sakamoto, M. Shirakawa, M. Ojima, A. Fujii, M. Ozaki, S. Shinkai, *J. Am. Chem. Soc.* **2007**, *129*, 4134.
- [3] F. Camerel, L. Bonardi, G. Ulrich, L. Charbonnière, B. Donnio, C. Bourgogne, D. Guillon, P. Retailleau, R. Ziessel, *Chem. Mater.* **2006**, *18*, 5009.
- [4] a) K. Murata, M. Aoki, T. Nishi, A. Ikeda, S. Shinkai, *J. Chem. Soc. Chem. Commun.* **1991**, 1715; b) S. R. Haines, R. G. Harrison, *Chem. Commun.* **2002**, 2846; c) M. Ayabe, T. Kishida, N. Fujita, K. Sada, S. Shinkai, *Org. Biomol. Chem.* **2003**, *1*, 2744.
- [5] a) H. Kobayashi, A. Friggeri, K. Koumoto, M. Amaike, S. Shinkai, D. N. Reinhoudt, *Org. Lett.* **2002**, *4*, 1423; b) H. Kobayashi, K. Koumoto, J. H. Jung, S. Shinkai, *J. Chem. Soc. Perkin Trans. 1* **2002**, *2*, 1930; c) S. van der Laan, B. L. Feringa, R. M. Kellogg, J. H. van Esch, *Langmuir* **2002**, *18*, 7136; d) J. H. Jung, S. Shinkai, T. Shimizu, *Nano Lett.* **2002**, *2*, 17; e) J. Mamiya, K. Kanie, T. Hiyama, T. Ikeda, T. Kato, *Chem. Commun.* **2002**, 1870; f) M. Moriyama, N. Mizoshita, T. Yokota, K. Kishimoto, T. Kato, *Adv. Mater.* **2003**, *15*, 1335.
- [6] J. J. D. de Jong, J. N. Lucas, R. M. Kellogg, J. H. van Esch, B. L. Feringa, *Science* **2004**, *304*, 278.
- [7] a) S. Wang, W. Shen, Y. Feng, H. Tian, *Chem. Commun.* **2006**, 1497; b) H. Tian, S. Wang, *Chem. Commun.* **2007**, 781.
- [8] H. Hachisako, I. Ihara, T. Kamiya, C. Hirayama, K. Yamada, *Chem. Commun.* **1997**, 19.
- [9] a) S. A. Ahmed, X. Sallenave, F. Fages, G. M. Gundert, W. M. Müller, U. Müller, F. Vögtle, J. L. Pozzo, *Langmuir* **2002**, *18*, 7096; b) A. R. Katritzky, R. Sakhuja, S. K. Khelashvili, *J. Org. Chem.* **2009**, *74*, 3062.
- [10] J. L. Pozzo, G. M. Clavier, J. P. Desvergne, *J. Chem. Mater.* **1998**, *8*, 2575.
- [11] K. Sugiyasu, N. Fujita, M. Takeuchi, S. Yamada, S. Shinkai, *Org. Biomol. Chem.* **2003**, *1*, 895.
- [12] a) R. J. Hovey, C. H. Fuchsman, N. Y. C. Chu, P. G. Piusz, photochromic compound, US Patent, 4215010, **1980**; b) R. J. Hovey, C. H. Fuchsman, N. Y. C. Chu, P. G. Piusz, US Patent, 3562172, **1982**; c) A. Kellmann, F. Tübel, R. Dubest, P. Levoir, *J. Photochem. Photobiol. A* **1989**, *49*, 63.
- [13] a) N. Y. C. Chu, *Can. J. Chem.* **1983**, *61*, 300; b) N. Y. C. Chu in *Photochromism: Molecules and Systems* (Eds.: H. Dürr, T. H. Bouas-Laurent), Elsevier, Amsterdam, **1990**, p. 879.
- [14] a) A. K. Chibisov, H. Görner, *J. Phys. Chem. A* **1999**, *103*, 5211; b) V. W. W. Yam, C. C. Ko, L. Wu, K. M. C. Wong, K. K. Cheung, *Organometallics* **2000**, *19*, 1820; c) A. V. Metelitsa, J. C. Micheau, N. A. Voloshin, E. N. Voloshina, V. I. Minkin, *J. Phys. Chem. A* **2001**, *105*, 8417; d) M. Querol, B. Bozic, N. Salluce, P. Belser, *Polyhedron* **2003**, *22*, 655; e) C. C. Ko, L. Wu, K. M. C. Wong, N. Zhu, V. W. W. Yam, *Chem. Eur. J.* **2004**, *10*, 766; f) R. T. F. Jukes, B. Bozic, F. Hartl, P. Belser, L. De Cola, *Inorg. Chem.* **2006**, *45*, 8326; g) Z. Bao, K. Y. Ng, V. W. W. Yam, C. C. Ko, N. Zhu, L. Wu, *Inorg. Chem.* **2008**, *47*, 8912; h) R. T. F. Jukes, B. Bozic, P. Belser, L. De Cola, F. Hartl, *Inorg. Chem.* **2009**, *48*, 1711.
- [15] a) G. Berkovic, V. Krongauz, V. Weiss, *Chem. Rev.* **2000**, *100*, 1741; b) V. Lokshin, A. Samat, A. V. Metelitsa, *Russ. Chem. Rev.* **2002**, *71*, 893; c) R. S. Becker, J. K. Roy, *J. Phys. Chem.* **1965**, *69*, 1435; d) J. Hobbey, F. Wilkinson, *J. Chem. Soc. Faraday Trans.* **1996**, *92*, 1323; e) F. M. Raymo, S. Giordani, *J. Org. Chem.* **2003**, *68*, 4158.

- [16] a) R. F. Khairutdinov, K. Giertz, J. K. Hurst, E. N. Voloshina, N. A. Voloshin, V. I. Minkin, *J. Am. Chem. Soc.* **1998**, *120*, 12707; b) R. A. Kopelman, S. M. Snyder, N. L. Frank, *J. Am. Chem. Soc.* **2003**, *125*, 13684.
- [17] H. Gong, C. Wang, M. Liu, M. Fan, *J. Mater. Chem.* **2001**, *11*, 3049.
- [18] a) C. S. Marvel, P. K. Porter, *Org. Synth.* **1941**, *1*, 411; b) M. Hosoda, EP 186364A2, **1986**; c) B. Osterby, R. D. McKelvey, L. Hill, *J. Chem. Educ.* **1991**, *68*, 424.
- [19] T. Ishi-i, R. Iguchi, E. Snip, M. Ikeda, S. Shinkai, *Langmuir* **2001**, *17*, 5825.
- [20] a) V. Percec, C. H. Ahn, T. K. Bera, G. Ungar, D. J. P. Yeardley, *Chem. Eur. J.* **1999**, *5*, 1070; b) V. Percec, M. Peterca, M. J. Sienkowska, M. A. Ilies, E. Aqad, J. Smidrkal, P. A. Heiney, *J. Am. Chem. Soc.* **2006**, *128*, 3324.

Received: January 20, 2010
Published online: June 25, 2010